

HORIZON: A High-Resolution Panorama Synthesis Framework

Kun Yan^{1*} Lei Ji² Chenfei Wu² Jian Liang³ Ming Zhou⁴ Nan Duan² Shuai Ma¹

¹SKLSDE Lab, Beihang University ²Microsoft Research Asia ³Peking University ⁴Langboat Technology
 {kunyan, mashuai}@buaa.edu.cn, {leiji, chewu, nanduan}@microsoft.com,
 j.liang@stu.pku.edu.cn, zhouting@chuangxin.com

Abstract

Panorama synthesis aims to generate a visual scene with all 360-degree views and enables an immersive virtual world. If the panorama synthesis process can be semantically controlled, we can then build an **interactive** virtual world and form an unprecedented human-computer interaction experience. Existing panoramic synthesis methods mainly focus on dealing with the inherent challenges brought by panoramas' spherical structure such as the projection distortion and the in-continuity problem when stitching edges, but is hard to effectively control semantics. The recent success of visual synthesis like DALL.E generates promising 2D flat images with semantic control, however, it is hard to directly be applied to panorama synthesis which inevitably generates distorted content. Besides, both of the above methods can not effectively synthesize high-resolution panoramas either because of quality or inference speed. In this work, we propose a new generation framework for high-resolution panorama images. The contributions include 1) alleviating the spherical distortion and edge in-continuity problem through spherical modeling, 2) supporting semantic control through both image and text hints, and 3) effectively generating high-resolution panoramas through parallel decoding. Our experimental results on a large-scale high-resolution Street View dataset validated the superiority of our approach quantitatively and qualitatively.

Introduction

Panoramic images and videos are becoming more and more popular and widely used, which provide an unlimited field of view (FOV) compared with planar images with a narrow FOV. Viewers can browse 360° views and shift the viewing from every direction with environmental details captured. Moreover, panoramic images also offer an immersive experience to viewers, which enables lots of interactive applications in a variety of domains including advertising, entertainment like gaming or designing industry, etc. However, panorama acquisition either requires intensive human efforts or special panoramic devices. Therefore, automatic panoramic synthesis becomes an emergent technique requirement with the development of virtual/augmented reality and devices like head-mounted displays or glasses. This technique can not only facilitate designers to save human efforts in creating and editing blueprints but also prevent the cost of special panoramic devices required.

*Contribution during internship at MSRA.

Panorama image has two unique characteristics: *spherical distortion* in distinct spatial location and *continuity* between the left most and right most boundaries compared with a planar image. Existing works on panoramic image synthesis mainly focus on generating a spherical image with a large FOV from one or a sequence of FOV images. Sumantri and Park (2020) introduced an equirectangular projection for realistic spherical image generation given multiple images, which aims to handle projection distortion problems when applying to flat images. Hara, Mukuta, and Harada (2021) generated a spherical image without discontinuity. Those methods lack the *user-controlled* capability, which is especially important in the virtual world synthesis.

Specifically, controlling the generated content with either style or semantic guidance plays a vital role in generating expected images. Particularly, a designer usually spends a lot of time creating and editing the image in the near field with a similar background but different semantics or styles. Inspired by human's capability of easily imagining 360-degree sceneries, there are research works to control the generation. Zhang et al. (2013) introduced image guidance for view extrapolation with similar scene categories and Karimi Dastjerdi et al. (2022) proposed a scene label guidance to control the style using a co-modulated GAN for 360° field of view extrapolation. Besides the view extrapolation task, panoramic image synthesis should take a variety of inputs to guide the generation process and provide a flexible way to apply this technique to many real applications. As shown in Figure 1, the user-controlling signal can be text description and/or visual input for semantic and style guidance.

Notably, recent methods of planar text to image generation including VAE (Ramesh et al. 2021), GAN (Esser, Rombach, and Ommer 2021) and Diffusion (Dhariwal and Nichol 2021) achieve great success in semantic relevance and magic-like controllability. These works can take various guidance as generating conditions by using Transformer's (Vaswani et al. 2017) capability. But all those methods are hard to be applied directly to panoramic image synthesis due to a lack of consideration of the spherical characteristics. All in all, no existing framework is general enough to handle all these spherical and controlling properties for the panorama in one unified framework. This motivates our work by combining the advanced guided image generation technique and designing specific modules, mechanisms,

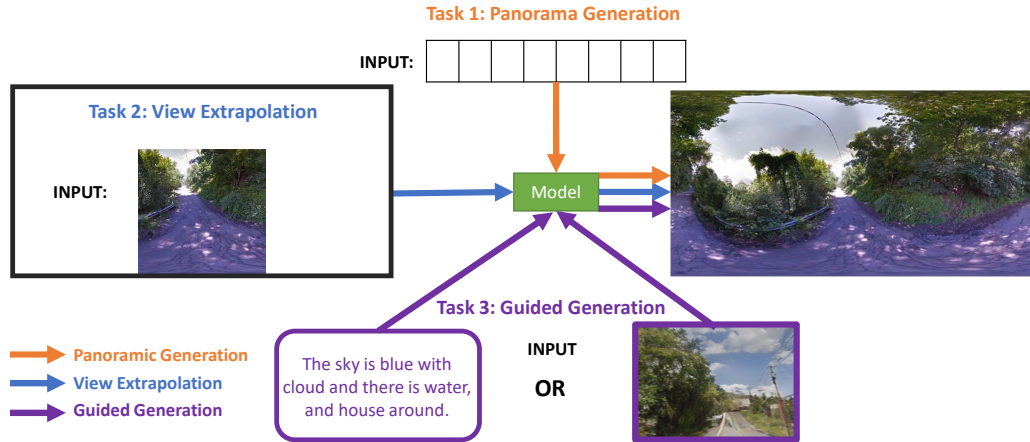


Figure 1: The task showcases.

and training strategies for spherical structures.

Furthermore, taking into account the actual application scenarios of panoramic images such as Virtual Reality and Augmented Reality, it is essential and necessary to generate *high-resolution* panoramic images so as to improve the immersive experience. However, existing panorama image generation methods rarely study the high-resolution capability. Moreover, the modish DALL-E-like works can not generate high-resolution panoramic images because of the spherical distortion and inference speed problems.

In this paper, we introduce a novel versatile framework to generate high-resolution panoramic images with a well-preserved spherical structure in conjunction with easy-to-use semantic controllability. In details, we adopt a two-stage procedure to learn an image encoder and decoder in the first step and a reconstruction model as the second step. Specifically, in the second stage, we design a new Spherical Parallel Modeling (SPM) method that not only maintains the efficiency of parallel decoding but also alleviates the local distortion problem through the spherical relative embedding and spherical conditioning improvement. Besides, we found that the panoramic pictures generated by SPM no longer have the problem of screen tearing when the left and right edges are spliced, which makes the generated panoramic pictures can be directly viewed in VR devices without subsequent editing.

The contributions can be summarized as:

- 1) alleviating the spherical distortion and edge discontinuity problem through spherical modeling,
- 2) supporting semantic control through both image and text hints
- 3) effectively generating high-resolution panoramas through parallel decoding. Experimental results demonstrate the effectiveness and efficiency of the model quantitatively and qualitatively.

Related Work

Panorama Synthesis 360 panorama synthesis is a long-standing task in the computer vision community. The related works can be categorized by inputs as a sequence of overlapped images (Szeliski 2006; Brown and Lowe 2007), sparse images (Sumantri and Park 2020) or a single image (Akimoto et al. 2019; Hara, Mukuta, and Harada 2021). Early attempts mainly adopt image *matching and stitching* methods (Szeliski 2006) to generate panorama given a sequence of overlapped image pieces. Later work exploited *generation models* to synthesize from a sequence of sparse images (Sumantri and Park 2020) or a single image (Akimoto et al. 2019; Koh et al. 2022) with known/unknown Field of View. The work (Akimoto et al. 2019; Koh et al. 2022) proposed a GAN-based method generation given one single image, and the paper (Rockwell, Fouhey, and Johnson 2021) adopt an autoregressive model for single-image scene synthesis.

Geometry and layout prediction, optical flow, depth and illumination estimation (Song and Funkhouser 2019; Xu et al. 2021; Zhang, Wang, and Liu 2022; Wang et al. 2022; Somanath and Kurz 2021) are widely studied for view synthesis in the computer graphics community. Besides, the **spherical structure and texture** are another intrinsic features to model for panorama synthesis. Existing works employed a cube map (Han and Suh 2020), cylinder convolution (Liao et al. 2022), predicted panoramic three-dimensional structure (Song et al. 2018) or considered scene symmetry (Hara, Mukuta, and Harada 2021) to extrapolate the 360 degree structure. These approaches are limited to handle *fixed* scenes and relative *low-resolution* images. Later, the work (Sumantri and Park 2020) introduced a hierarchical synthesis network on small, medium, and high resolution, and similarly, another work (Akimoto, Matsuo, and Aoki 2022) employed U-net structure for high resolution. Compared with 1024*512 at most in these previous works, our work is able to handle even higher resolution of

1536*768.

Additionally, **user-controlled** semantic content generation is also important for interactive panorama generation. Recent works adopt scene symmetry (Hara, Mukuta, and Harada 2021) using the CVAE-base method or scene category (Karimi Dastjerdi et al. 2022) with GAN-based methods as guidance for view extrapolation. However, none existing framework is general enough to handle all *spherical*, *user-controlling* and *high-resolution* properties for the panorama in one unified framework. Thus we introduce a versatile framework and design various mechanisms to handle a spherical distortion or continuity. Moreover, the two-stage network is able to generate high-resolution spherical images and is flexible enough to plug in semantic guidance without further tuning.

Image Generation Previous image generation works mainly adopt the generative adversarial networks(GAN) (Goodfellow et al. 2014; Reed et al. 2016; Xu et al. 2018; Qiao et al. 2019; Zhang et al. 2021a), VAE-based method (Kingma and Welling 2013; van den Oord, Vinyals, and kavukcuoglu 2017), and denoising diffusion models (Nichol et al. 2021; Gu et al. 2021; Kim and Ye 2021). With the development of the transformer model, one of the emerging research directions is the two-stage method, which is a new paradigm for pretraining with web-scale image and text pairs. They demonstrated the pretrained models are effective in generalizing high semantically related open-domain images, which first adopt VQVAE (van den Oord, Vinyals, and kavukcuoglu 2017)/VAGAN (Esser, Rombach, and Ommer 2021) to tokenize images into discrete tokens and then generate these visual tokens for further decoding to real images (Ramesh et al. 2021; Ding et al. 2021; Zhang et al. 2021b). Esser, Rombach, and Ommer (2021); Chang et al. (2022); Wu et al. (2022) devote effort to high-resolution planer image generation, but their results can not fit the need of panoramic scenarios, as they always produce blurred or teared artifacts more or less. Although guided image generation achieves superior performance (Ramesh et al. 2021; Ding et al. 2021; Zhang et al. 2021b), it is hard to directly apply the existing models for a panoramic generation without consideration of the unique spherical structure.

Method

The overall training is a two-stage procedure, similar to (Ramesh et al. 2021; Ding et al. 2021). The first stage is to train an encoder for image/view representation (discrete visual tokens in this paper) and a decoder for image generation, both of which are frozen in the second stage. The second stage is to learn a reconstruction model based on the discrete visual representation. The details are illustrated below and also presented in Figure 2.

- **Stage 1.** Every equirectangular projected panoramic image with a resolution of 768x1,536 is first divided into 3x6=18 RGB view patches, each with a resolution of 256x256. Then we train a VQGAN(Esser, Rombach, and Ommer 2021) on every view patch separately. The encoder of VQGAN compresses each RGB view patch into

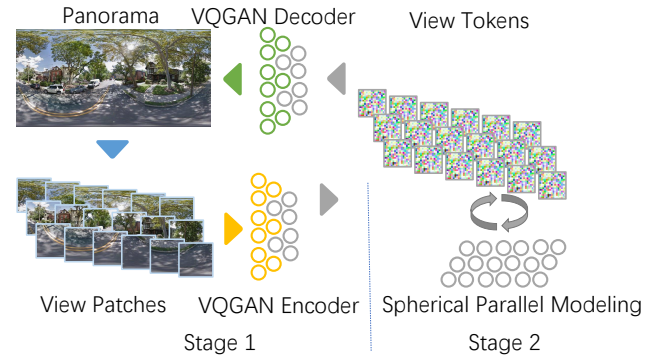


Figure 2: Given a high-resolution panoramic image, equally divide into 3x6=18 view patches. In the first stage, we train VQGAN for each of the 18 view patches separately. Specifically, each view patch is encoded into 16x16 view tokens by using VQGAN Encoder. In the second stage, the newly proposed spherical parallel model is designed to reconstruct the overall view tokens and synthesize the panoramic image by using VQGAN Decoder.

a 16x16 grid of view tokens. The overall view token dictionary has a size of 16,384 possible values. As a result, each panoramic image has 18x16x16 view tokens.

- **Stage 2.** All 18 groups of view tokens from a single panoramic image are modeled as a whole context to incrementally learn the reconstruction of all view tokens. The reconstruction models include autoregressive modeling, local parallel modeling, and the newly proposed spherical parallel modeling detailed described in the following subsections.

We apply the off-the-shelf model in the first stage and mainly devote our effort to effectively modeling the prior in the second stage. Due to the large number of view tokens for a single panorama (18x16x16=4068), it is still a non-trivial problem to learn the reconstruction. We should balance the quality, efficiency, and controllability with considerable virtuosity. In the following subsections, we will describe our progressive attempts and corresponding design considerations.

Auto-Regressive Modeling

The most intuitive way is to directly employ a transformer decoder to generate 4068 view tokens one by one, which is also our first attempt. However, we quickly discovered the defects of this scheme. Due to the quadraticity of the attention mechanism of the transformer itself, directly inputting 4068 tokens into the model will bring huge memory consumption and great difficulties to the training of the model. At the same time, the sequence is too long for the model to converge effectively.

After deduction, we noticed that the dependence between tokens becomes weak or even negative as the relative distance increases. Therefore, we shrink the attention scope for both efficiency and effectiveness. Specifically, the range of attention for each view patch is limited to 2 surrounding

view patches on the left and above, and autoregressively performs the prediction within the current patch. The interval of attention is shown at the top of Figure 3. After making this improvement, we have been able to generate decent high-resolution panoramas, which are also used as our first baseline **ARM**.

Local Parallel Modeling

Although the improved version of **ARM** makes high-resolution panorama generation basically feasible, flattening the view patch into a one-dimensional sequence of tokens in raster scan order is still not an optimal and efficient modeling solution. Since the length of the autoregressive sequence still grows quadratically, it not only presents a challenge for modeling long-term correlations but also makes decoding intractable. Inspired by MaskGIT(Chang et al. 2022), we adopt the Masked Visual Token Modeling(MVTM) into the view modeling process, which can be formulated as:

$$\mathcal{L}_{LPM} = -\mathbb{E} \left[\sum_{\forall i \in [1, N], \text{mask}_i=1} \log p(y_i | Y_{\overline{M}}; Y_W) \right] \quad (1)$$

For every training pass, sample a subset of tokens and replace them with a special [MASK] token. The sampling procedure is parameterized by a mask scheduling function $\lceil \cos(r * \pi/2) \cdot N \rceil$, r is a real number uniformly sampled from 0 to 1, N is the total number of view tokens in current view patch. Masked token sequence $Y_{\overline{M}}$ and ground truth view tokens from surrounding view patch Y_W are fed into a multi-layer bidirectional transformer to predict the probabilities $p(y_i | Y_{\overline{M}}; Y_W)$ for each masked token, where the negative log-likelihood is computed as the cross-entropy between the ground-truth and prediction.

During inference, we use a similar iterative decoding technique with a constant step T , initially all tokens in the current patch are masked, at each step t only $\lceil (1 - \cos(\frac{\pi t}{2T}))N \rceil$ tokens with higher confidence are kept, others will be refined during further steps. We named this adapted version of MaskGIT as Local Parallel Modeling(**LPM**), because for each local view patch the modeling is applied in parallel. By applying this strategy, we shorten the inference speed by 64 times. However, we also observe a significant performance drop compared with **ARM**. This also drives us to conduct further investigation and methodological improvement.

Spherical Parallel Modeling

So far, we have not taken the spherical characteristics of panoramic images into consideration in model design but treated each patch view equally, assuming that its visual features after spherical projection are translation-invariant on the two-dimensional plane. This is obviously not in line with the actual situation. We observed that under the **ARM** method, the model can still maintain a strong relative positional relationship, and according to the current sequence order, it can be deduced what degree of deformation should be used to generate the current view token. However, under the **LPM** method, the generation of the current token

is no longer strictly constrained by the previous token, and sequence order is no longer an important factor for model learning goals. Naturally, the panoramic images generated by **LPM** have distorted local details, which are relatively weak in performance indicators such as FID.

In this section, we describe a new Spherical Parallel Modeling(**SPM**) method that not only maintains the efficiency of parallel decoding but also alleviates the local distortion problem through the spherical relative embedding and spherical conditioning improvement. Besides, we found that the panoramic pictures generated by **SPM** no longer have the problem of screen tearing when the left and right edges are spliced, which makes the generated panoramic pictures can be directly viewed in VR devices without subsequent editing.

Spherical Relative Embedding Relative positional embedding has been shown effectively capture the relative positional information during the attention process. More formally, a positional encoding function $f(\mathbf{x}, l)$ for an item x and its position l such that, for two items \mathbf{q} and \mathbf{k} at positions m and n , the inner product between $f(\mathbf{q}, m)$ and $f(\mathbf{k}, n)$ is sensitive only to the values of \mathbf{q} , \mathbf{k} , and their relative position $m - n$. The dot product between two vectors is a function of the magnitude of individual vectors and the angle between them. Starting from here, RoPE(Su et al. 2021) is proposed to represent the token embeddings as complex numbers and their positions as pure rotations that apply to them. If both the query and key are shifted by the same amount, changing absolute position but not relative position, this leads both representations to be additionally rotated in the same manner thus the angle between them remains unchanged and the dot product also remain unchanged. One of the function solutions that satisfies the above requirement can be formulated as below:

$$\begin{aligned} f(\mathbf{q}, m) &= \begin{pmatrix} M_1 & & & \\ & M_2 & & \\ & & \ddots & \\ & & & M_{d/2} \end{pmatrix} \begin{pmatrix} q_1 \\ q_2 \\ \vdots \\ q_d \end{pmatrix} \quad (2) \\ &= \mathbf{R}_m \mathbf{Q}_m \\ &= \mathbf{R}_m \mathbf{W}_q \mathbf{X}_m \end{aligned}$$

where $M_j = \begin{pmatrix} \cos m\theta_j & -\sin m\theta_j \\ \sin m\theta_j & \cos m\theta_j \end{pmatrix}$, \mathbf{R}_m is the block diagonal rotation matrix, \mathbf{W}_q is the learned query weights, and \mathbf{X}_m is the embedding of the m -th token. For query \mathbf{k} , a similar corresponding equation is applied, too. When extending to the 2-dimensional case, the rotation matrix should correlate with both coordinates x and y :

$$M_{x,y} = \begin{pmatrix} \cos x\theta & -\sin x\theta & 0 & 0 \\ \sin x\theta & \cos x\theta & 0 & 0 \\ 0 & 0 & \cos y\theta & -\sin y\theta \\ 0 & 0 & \sin y\theta & \cos y\theta \end{pmatrix} \quad (3)$$

However, only two-dimensional relative position embedding cannot represent the relative positional relationship of the spherical surface. This is manifested in two aspects. One

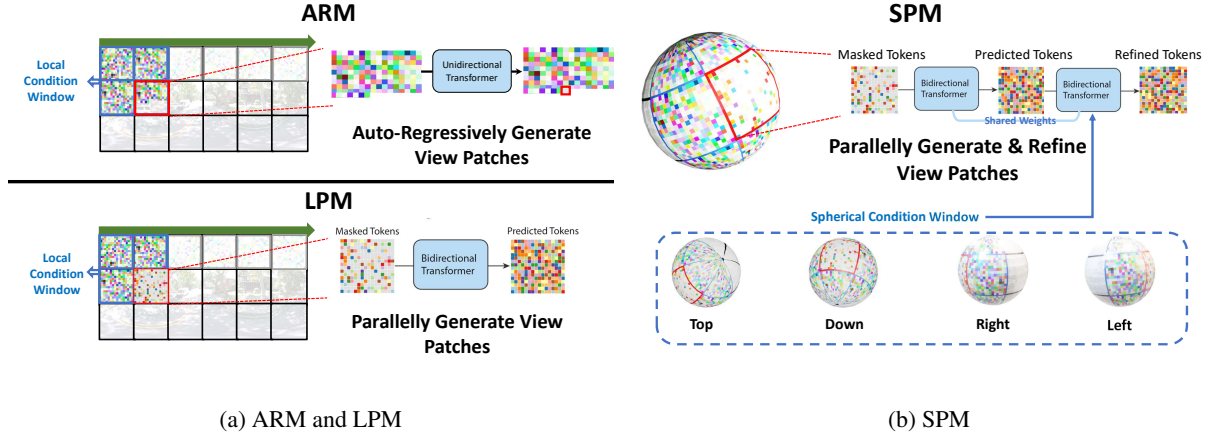


Figure 3: Modeling Strategy: we progressively improve modeling strategy from ARM to LPM and eventually SPM, achieving both high efficiency and high fidelity. In this Figure, the red boxes show the current view patch to be generated, while the blue boxes present the condition window.

is that the distance between the plane and the spherical surface is measured in different ways. Second, the coordinates of the same latitude have a ring-shaped positional relationship, that is, for a token sequence $0 \dots m$ at the same latitude, the positional embedding of token 0 and the positional embedding of token m should be as close as possible. To satisfy this property, we re-derived the rotation matrix, instead of the Θ in the original RoPE(Su et al. 2021):

$$\Theta = \left\{ \theta_i = 10000^{-2(i-1)/d}, i \in [1, 2, \dots, d/2] \right\} \quad (4)$$

We define Θ_{sphere} as:

$$\Theta_{sphere,x} = \left\{ \theta_i = \frac{-2(i-1) * 2\pi}{d * w}, i \in [1, 2, \dots, d/2] \right\}, \quad (5)$$

$$\Theta_{sphere,y} = \left\{ \theta_i = \frac{-2(i-1) * \pi}{d * h}, i \in [1, 2, \dots, d/2] \right\}, \quad (6)$$

where x, y are the different axis of the spherical surface, w is the length of token sequences along the x axis, and h is the length along the y axis. Note that as $\Theta_{sphere,x}$ represents latitude, the molecular has a factor 2π , which makes the rotation of the sequence head and tail as close as possible. While $\Theta_{sphere,y}$ does not keep this property, as the poles of a sphere are far from each other naturally.

Spherical Relative Embedding(SRE) applies to self-attention as follows:

$$SRE(\mathbf{q}_{(x1,y1)}^\top) SRE(\mathbf{k}_{(x2,y2)}) = \left(\mathbf{R}_{\Theta,(x1,y1)}^d \mathbf{W}_q \mathbf{x}_{(x1,y1)} \right)^\top \left(\mathbf{R}_{\Theta,(x2,y2)}^d \mathbf{W}_k \mathbf{x}_{(x2,y2)} \right) \quad (7)$$

Spherical Conditioning To generate continuity of the horizontal boundary, the autoregressive one-directional transformer decoder generates the tokens from left to right,

which leads to in-continuity between the left-most and right-most boundaries. When viewing these images with the panorama viewer, we see obvious tearing artifacts at the stitching seams. To make the left-most and right-most pixels consistent, these pixels should be generated with consideration of each other. This local detail also implies a deeper defect of the aforementioned method. that is, if the context information of the complete spherical structure is not considered when predicting the token of the current position, the consistency and integrity of the final overall result cannot be guaranteed.

In order to fix this defect, we redesigned the conditions for generating each view patch. Through the two-pass mechanism, the model no longer only autoregressively focuses on the small window on the upper left but focuses on the entire hemispherical area around the current patch view. Specifically, in the training phase, the model learns both \mathcal{L}_{LPM} and \mathcal{L}_{SPM} in each iteration step. The form of \mathcal{L}_{SPM} is as follows:

$$\mathcal{L}_{SPM} = -\mathbb{E} \left[\sum_{\forall i \in [1, N], mask_i = 1} \log p(y_i | Y_{\overline{M}}; Y_S) \right] \quad (8)$$

It is worth noting that Y_S is different from Y_W in \mathcal{L}_{LPM} . For the view patch at row i and column j , the corresponding Y_W contains view patches of upper and left, while Y_S contains these of upper, down, left, and right. Specifically, Y_S comprises of $[(i-1, j), (i, j-1), (i-1, j-1)]$, and Y_S comprises of $[(i-1, j-1), (i-1, j), (i-1, j+1), (i, j-1), (i, j+1), (i+1, j-1), (i+1, j), (i+1, j+1)]$. When the above coordinates are out of bounds, Y_W will not consider the part beyond the boundary, and Y_S will extend the part beyond the x-axis to the other side. In addition, each Y_S also applies the spherical relative embedding transformation described above and a special learnable phase embedding \mathbf{I} to let the model know which pass it is currently in.

During inference, the model first performs a complete

LPM decoding and retains all tokens, and then superimposes the spherical relative embedding and phase embedding I for each token in the second pass to optimize the generation result of the first pass. This method only increases the inference time by 1 time, which is still faster than ARM, but can greatly improve the generation quality, surpassing ARM and LPM.

Guided Semantic-Condition To further enhance the capabilities of the model, we try to use semantics as an additional input condition to guide the panoramic image generation process. Specifically, we use FOV=90 degrees to cut out the front, back, left, and right perspective pictures of the panoramic image and encode them with the pretrained CLIP(Radford et al. 2021) visual module to get four semantic vectors for each panorama. We then take those vectors as semantic conditions sequentially appended to sphere conditions, and train in an end-to-end way. Similarly, we also employ the pretrained CLIP text module to encode text as a semantic condition to control the generation. During inference, we can either input visual hints or text hints respectively.

Experiment Setup

Dataset

We validate our model on the StreetLearn dataset(Mirowski et al. 2019), which is a set of Google Street View panoramas images with high resolution. Specifically, we adopt Pittsburgh data containing 58k images. The data is split into 52.2k for training and 5.8k for tests. The equirectangular panorama RGB images are stored in compressed high-quality JPEG format with sizes of 1664 x 832. For our setting, we resize all panoramas into 1536x768. We run our experiment on 64 V100 GPUs, each with 32GiB memory. We evaluate our model on three typical panorama image generation, view extrapolation, and controlled generation tasks.

Task 1: Panorama Generation

To evaluate the image quality, the Frchet inception distance FID score (Heusel et al. 2017) is the widely used evaluation metric. FID measures feature distribution distance by comparing the mean and standard deviation between real and fake images. However, we argue the typical FID treats every position of the image equally while the information density of the spherical image varies upon spatial position. In fact, the top and bottom of the image represent sparse information like sky or ground while the middle of the image shows intensive information with high density. Considering the spherical structure, we propose a novel *spherical FID* to evaluate the quality of panoramic images, which dynamically evaluates the image quality with regard to the variety of information density. Specifically, FID is calculated on various view patch sets of an image. Given a grid of 3 rows and 6 columns of view patches for a panorama, we name each row as top, middle and bottom respectively, and calculate the FID scores on those three subsets. We report the sphericalFID score of different locations respectively in Table 1. From the table we can see, that our SPM(+SRE+SC) model can generate State-of-the-art results and outperforms baseline models

to a large extent. Both the spherical relative embedding and spherical conditioning are effective mechanisms. Considering the efficiency, LPM is the most efficient model but with almost the worst performance. The second pass revises the first pass with the tradeoff between efficiency and effectiveness.

We present several examples generated in Figure 4. We rely on the open tool Online 360° Panorama Viewer VR ¹ to view the image. For each case, we present the snapshot of the four views from left to right in the Figure. More cases are listed in the appendix.

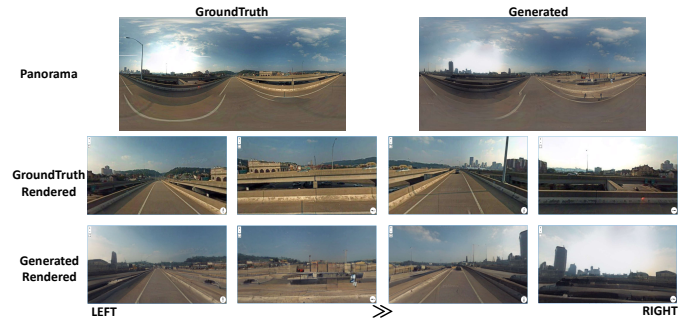


Figure 4: Generated examples. The first row presents the ground-truth and SPM-generated images. The second and third rows are the four snapshots of ground truth and our results respectively by using the 360 panorama viewers.

View In-continuity Problem The in-continuity of synthesis occurs when the left-most and the right-most boundary merged into one spherical image. Among the four snapshots from the viewer tool, the last (4th) image rendered is the merged image and the middle is exactly the boundary between the left most and right most. From the showcases in Figure 5 we can see, that the results of the baseline algorithm have an obvious separator in the middle while our algorithm considering the spherical attention generate a smooth connection. This demonstrates the effectiveness of our proposed spherical attention module.



Figure 5: In-continuity v.s. Continuity. The three randomly selected cases present results from baseline and our models. The top images are the generated images of the baseline(LPM) method and the bottom examples are from our model(SPM). There is an obvious split line in the middle of each image on the top examples while the boundary is smooth on the bottom examples.

¹<https://renderstuff.com/tools/360-panorama-web-viewer/>

	Spherical FID↓				Efficiency↓
	mean	top	middle	bottom	Forward
ARM	41.21	26.16	32.17	65.32	4068
LPM	57.13	64.34	46.71	60.35	144
SPM(+SRE)	39.18	28.72	26.44	62.39	288
SPM(+SRE+SC)	20.97	15.82	21.80	25.29	288

Table 1: Generation Results. SPM is the spherical model in our paper, SRE is spherical relative embedding and SC is spherical conditioning.

	$SSIM \uparrow$	$PSNR \uparrow$
ARM	0.521	15.39
LPM	0.508	14.94
SPM	0.542	15.49

Table 2: View Extrapolation Results.

Task 2: View Extrapolation

We conduct quantitative experiments and adopt structural similarity (SSIM) and peak-to-signal-noise-ratio (PSNR) as evaluation metrics specific for the view extrapolation tasks. The structural similarity index is calculated on various windows of an image, and is based on three comparison measurements between the generated and the reference images: luminance, contrast, and structure. The peak-to-signal-noise-ratio (PSNR) measures the difference in the pixel values, which is to calculate the Mean Square Error between the generated and the reference images. From the results in Table 2, our model achieves the best performance compared with the baseline methods.

Besides, we also show several examples of view extrapolation in Figure 6. From the results, we found our model tends to generate *symmetric* texture as shown in the first and third cases. Both cases have *silent* objects (“trees” in the first case and “building” in the third case) on the right part and the whole image is predominated. While the second case has a clue of the “white building” on the left and the “grass and lights” on the right, and generates different textures for the left and right respectively. All three cases demonstrate the capability of our model in generating reasonable and high-resolution panoramas. Despite that, there is still the low quality of small objects like “cars” and the details as shown in the third case, which can be future work.

Task 3: Guided Generation

We illustrate the guided generation showcases in Figure 7 and Figure 8. The visual guidance and text guidance are encoded by CLIP model.

Visual Guidance As shown in Figure 7, there are 3 cases presenting the results given the visual guidance. For case (a), the left case shows the original panoramic image (bottom) as well as 4 FOV images rendered (top 4 images). The middle and right cases demonstrate the generated results given the 4th guided image highlighted in the **red box**. The middle case edits the final view with “a single tree”, and the right case edits the final view with “lush trees”. For case (b) and case (c), we can see the controlled image has a “red house” and “yellow house” respectively. This demon-

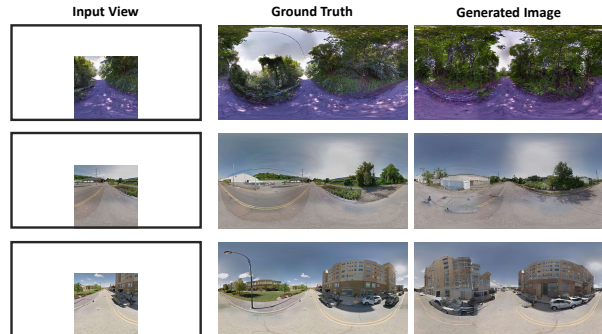


Figure 6: View Extrapolation. The first column gives the input samples, the second column presents the ground truth examples, and the third column demonstrates the generated panorama.

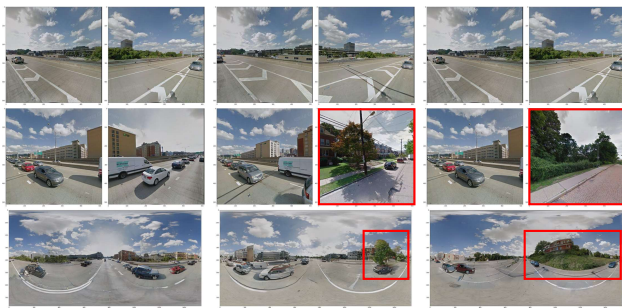
strates the model is capable of generating panoramic images with both semantic and style controls. Please note, in order to generate a consistent image, the context view may be changed accordingly.

Text Guidance As shown in Figure 8, there are 4 cases presenting the results given the 4 different text guidance. For each case, the first row contains the original panorama images, the second row presents the text guidance and the third row illustrates the generated panoramic images. As shown in these cases, the highlighted **red box** shows the corresponding region generated. For semantic guidance, we can see the “cracked roads” in Case (a), “lush trees” in Case (b), “clear sky” in Case (c), and “red house” in case (d).

From these examples, we can observe that our framework can edit and modify semantic elements in the panorama by providing reference view images or text hints at specific locations. More cases can be found in the appendix.

Conclusion

Panorama synthesis is an extremely promising and challenging topic at the moment, and it is also the core foundational technology of the upcoming meta-verse immersive experience. Inspired by the recent advances in the general framework for planar image generation, in this paper, we introduce a novel versatile framework to generate high-resolution panoramic images with a well-preserved spherical structure in conjunction with easy-to-use semantic controllability. The contributions include 1) alleviating the spherical distortion and edge in-continuity problem through spherical modeling, 2) supporting semantic control through both image and text



(a)



(b)



(c)

Figure 7: Visual Guided generation. When we replace the guidance with different visual semantics as shown in the middle and right columns, we can manipulate the generated panoramas as we need.



↓ The roads lay cracked and brittle like old dinosaur skin set out to bake in the sun. ↓



(a)



↓ Lush trees grow on the side of the street ↓



(b)



↓ The sky is clear, and the bright sun shines ↓



(c)



↓ Beautiful red house on the roadside. ↓



(d)

Figure 8: Textual Guided generation. We can also use natural language to edit or embellish target panoramas. In each case, the top row are the original panoramas, and the bottom row are the embellished panoramas according to the text hint shows in the middle.

hints, and 3) effectively generating high-resolution panoramas through parallel decoding. This hopefully builds a new paradigm for panorama synthesis. In future work, further guidance can be involved in the generation to enhance the interactive experience. When we greatly improve the infer-

ence speed, the model will be able to directly replace the existing human-built interface, bringing unprecedented application changes.

References

- Akimoto, N.; Kasai, S.; Hayashi, M.; and Aoki, Y. 2019. 360-degree image completion by two-stage conditional gans. In *2019 IEEE International Conference on Image Processing (ICIP)*, 4704–4708. IEEE.
- Akimoto, N.; Matsuo, Y.; and Aoki, Y. 2022. Diverse Plausible 360-Degree Image Outpainting for Efficient 3DCG Background Creation. In *Proceedings of the IEEE/CVF Conference on Computer Vision and Pattern Recognition*, 11441–11450.
- Brown, M.; and Lowe, D. G. 2007. Automatic panoramic image stitching using invariant features. *International journal of computer vision*, 74(1): 59–73.
- Chang, H.; Zhang, H.; Jiang, L.; Liu, C.; and Freeman, W. T. 2022. MaskGIT: Masked Generative Image Transformer. *ArXiv*, abs/2202.04200.
- Dhariwal, P.; and Nichol, A. 2021. Diffusion models beat gans on image synthesis. *Advances in Neural Information Processing Systems*, 34.
- Ding, M.; Yang, Z.; Hong, W.; Zheng, W.; Zhou, C.; Yin, D.; Lin, J.; Zou, X.; Shao, Z.; Yang, H.; et al. 2021. Cogview: Mastering text-to-image generation via transformers. *Advances in Neural Information Processing Systems*, 34: 19822–19835.
- Esser, P.; Rombach, R.; and Ommer, B. 2021. Taming transformers for high-resolution image synthesis. In *Proceedings of the IEEE/CVF Conference on Computer Vision and Pattern Recognition*, 12873–12883.
- Goodfellow, I.; Pouget-Abadie, J.; Mirza, M.; Xu, B.; Warde-Farley, D.; Ozair, S.; Courville, A.; and Bengio, Y. 2014. Generative adversarial nets. *Advances in neural information processing systems*, 27.
- Gu, S.; Chen, D.; Bao, J.; Wen, F.; Zhang, B.; Chen, D.; Yuan, L.; and Guo, B. 2021. Vector quantized diffusion model for text-to-image synthesis. *arXiv preprint arXiv:2111.14822*.
- Han, S. W.; and Suh, D. Y. 2020. PIINET: A 360-degree Panoramic Image Inpainting Network Using a Cube Map. *arXiv preprint arXiv:2010.16003*.
- Hara, T.; Mukuta, Y.; and Harada, T. 2021. Spherical Image Generation from a Single Image by Considering Scene Symmetry. In *Proceedings of the AAAI Conference on Artificial Intelligence*, volume 35, 1513–1521.
- Heusel, M.; Ramsauer, H.; Unterthiner, T.; Nessler, B.; and Hochreiter, S. 2017. GANs Trained by a Two Time-Scale Update Rule Converge to a Local Nash Equilibrium. In *NIPS*.
- Karimi Dastjerdi, M. R.; Hold-Geoffroy, Y.; Eisenmann, J.; Khodadadeh, S.; and Lalonde, J.-F. 2022. Guided Co-Modulated GAN for 360° Field of View Extrapolation. *arXiv e-prints*, arXiv-2204.
- Kim, G.; and Ye, J. C. 2021. Diffusionclip: Text-guided image manipulation using diffusion models. *arXiv preprint arXiv:2110.02711*.
- Kingma, D. P.; and Welling, M. 2013. Auto-encoding variational bayes. *arXiv preprint arXiv:1312.6114*.
- Koh, J. Y.; Agrawal, H.; Batra, D.; Tucker, R.; Waters, A.; Lee, H.; Yang, Y.; Baldrige, J.; and Anderson, P. 2022. Simple and Effective Synthesis of Indoor 3D Scenes. *arXiv preprint arXiv:2204.02960*.
- Liao, K.; Xu, X.; Lin, C.; Ren, W.; Wei, Y.; and Zhao, Y. 2022. Cylind-Painting: Seamless 360 {deg} Panoramic Image Outpainting and Beyond with Cylinder-Style Convolutions. *arXiv preprint arXiv:2204.08563*.
- Mirowski, P.; Banki-Horvath, A.; Anderson, K.; Teplyashin, D.; Hermann, K. M.; Malinowski, M.; Grimes, M. K.; Simonyan, K.; Kavukcuoglu, K.; Zisserman, A.; et al. 2019. The streetlearn environment and dataset. *arXiv preprint arXiv:1903.01292*.
- Nichol, A.; Dhariwal, P.; Ramesh, A.; Shyam, P.; Mishkin, P.; McGrew, B.; Sutskever, I.; and Chen, M. 2021. Glide: Towards photorealistic image generation and editing with text-guided diffusion models. *arXiv preprint arXiv:2112.10741*.
- Qiao, T.; Zhang, J.; Xu, D.; and Tao, D. 2019. Mirrorgan: Learning text-to-image generation by redescription. In *Proceedings of the IEEE/CVF Conference on Computer Vision and Pattern Recognition*, 1505–1514.
- Radford, A.; Kim, J. W.; Hallacy, C.; Ramesh, A.; Goh, G.; Agarwal, S.; Sastry, G.; Askell, A.; Mishkin, P.; Clark, J.; et al. 2021. Learning transferable visual models from natural language supervision. In *International Conference on Machine Learning*, 8748–8763. PMLR.
- Ramesh, A.; Pavlov, M.; Goh, G.; Gray, S.; Voss, C.; Radford, A.; Chen, M.; and Sutskever, I. 2021. Zero-shot text-to-image generation. In *International Conference on Machine Learning*, 8821–8831. PMLR.
- Reed, S.; Akata, Z.; Yan, X.; Logeswaran, L.; Schiele, B.; and Lee, H. 2016. Generative adversarial text to image synthesis. In *International Conference on Machine Learning*, 1060–1069. PMLR.
- Rockwell, C.; Fouhey, D. F.; and Johnson, J. 2021. Pixel-synth: Generating a 3d-consistent experience from a single image. In *Proceedings of the IEEE/CVF International Conference on Computer Vision*, 14104–14113.
- Somanath, G.; and Kurz, D. 2021. HDR Environment Map Estimation for Real-Time Augmented Reality. In *Proceedings of the IEEE/CVF Conference on Computer Vision and Pattern Recognition*, 11298–11306.
- Song, S.; and Funkhouser, T. 2019. Neural illumination: Lighting prediction for indoor environments. In *Proceedings of the IEEE/CVF Conference on Computer Vision and Pattern Recognition*, 6918–6926.
- Song, S.; Zeng, A.; Chang, A. X.; Savva, M.; Savarese, S.; and Funkhouser, T. 2018. Im2pano3d: Extrapolating 360 structure and semantics beyond the field of view. In *Proceedings of the IEEE Conference on Computer Vision and Pattern Recognition*, 3847–3856.

Su, J.; Lu, Y.; Pan, S.; Wen, B.; and Liu, Y. 2021. RoFormer: Enhanced Transformer with Rotary Position Embedding. *arXiv preprint arXiv:2104.09864*.

Sumantri, J. S.; and Park, I. K. 2020. 360 panorama synthesis from a sparse set of images with unknown field of view. In *Proceedings of the IEEE/CVF Winter Conference on Applications of Computer Vision*, 2386–2395.

Szeliski, R. 2006. Image alignment and stitching: a tutorial, foundations and trends in computer graphics and computer vision. *Now Publishers*, 2(1): 120.

van den Oord, A.; Vinyals, O.; and Kavukcuoglu, K. 2017. Neural Discrete Representation Learning. In Guyon, I.; Luxburg, U. V.; Bengio, S.; Wallach, H.; Fergus, R.; Vishwanathan, S.; and Garnett, R., eds., *Advances in Neural Information Processing Systems*, volume 30. Curran Associates, Inc.

Vaswani, A.; Shazeer, N.; Parmar, N.; Uszkoreit, J.; Jones, L.; Gomez, A. N.; Kaiser, Ł.; and Polosukhin, I. 2017. Attention is all you need. *Advances in neural information processing systems*, 30.

Wang, G.; Yang, Y.; Loy, C. C.; and Liu, Z. 2022. Style-Light: HDR Panorama Generation for Lighting Estimation and Editing. *arXiv preprint arXiv:2207.14811*.

Wu, C.; Liang, J.; Hu, X.; Gan, Z.; Wang, J.; Wang, L.; Liu, Z.; Fang, Y.; and Duan, N. 2022. NUWA-Infinity: Autoregressive over Autoregressive Generation for Infinite Visual Synthesis.

Xu, J.; Zheng, J.; Xu, Y.; Tang, R.; and Gao, S. 2021. Layout-guided novel view synthesis from a single indoor panorama. In *Proceedings of the IEEE/CVF Conference on Computer Vision and Pattern Recognition*, 16438–16447.

Xu, T.; Zhang, P.; Huang, Q.; Zhang, H.; Gan, Z.; Huang, X.; and He, X. 2018. AttnGAN: Fine-Grained Text to Image Generation with Attentional Generative Adversarial Networks. *2018 IEEE/CVF Conference on Computer Vision and Pattern Recognition*, 1316–1324.

Zhang, H.; Koh, J. Y.; Baldrige, J.; Lee, H.; and Yang, Y. 2021a. Cross-Modal Contrastive Learning for Text-to-Image Generation. In *CVPR*.

Zhang, W.; Wang, Y.; and Liu, Y. 2022. Generating High-Quality Panorama by View Synthesis Based on Optical Flow Estimation. *Sensors*, 22(2): 470.

Zhang, Y.; Xiao, J.; Hays, J.; and Tan, P. 2013. Framebreak: Dramatic image extrapolation by guided shift-maps. In *Proceedings of the IEEE Conference on Computer Vision and Pattern Recognition*, 1171–1178.

Zhang, Z.; Ma, J.; Zhou, C.; Men, R.; Li, Z.; Ding, M.; Tang, J.; Zhou, J.; and Yang, H. 2021b. M6-UFC: Unifying Multi-Modal Controls for Conditional Image Synthesis. *arXiv preprint arXiv:2105.14211*.

Implementation Details

The number of transformer layers is 24, all those layers are with 20 attention heads and a hidden size of 1280. The dropout rate for attention and feed-forward is 0.1. We update the parameters using AdamW with $\beta_1=0.9$, $\beta_2=0.96$, $\epsilon = 1e-8$, and weight decay multiplier $4.5e-2$. We clip the de-compressed gradients by norm using a threshold of 4, prior to applying the Adam update. Gradient clipping is only triggered during the warm-up phase at the start of training. We trained the model using 64 NVIDIA V100 GPUs each with 32GB memory and a total batch size of 256, for a total of 20 epochs, which is about 4K steps. At the start of training, we use a linear schedule to ramp up the learning rate to $1e-4$ over 5000 updates and reduce the learning rate to 0 in a cosine schedule.

Semantic Control Samples

By replacing the visual conditions, we can control the semantics of the generated panoramas. As the cases below, in each sub-figure, the top four images are come from the real view, and will be encoded as semantic condition using CLIP, feeding into our model. When we replace part of the conditions, we can observe that the model will adjust the output to fit the semantic needs (marked with red boxes). Thus we can manipulate and control the panoramas on our needs.



(a)

More Samples



(c)



(d)



(e)



(f)



(g)



(h)



(i)



(j)



(k)



(l)



(m)



(n)

HORIZON:A New High Resolution Panorama Synthesis Framework

Anonymous submission

Implementation Details

The number of transformer layers is 24, all those layers are with 20 attention heads and a hidden size of 1280. The dropout rate for attention and feed-forward is 0.1. We update the parameters using AdamW with $\beta_1=0.9$, $\beta_2=0.96$, $\epsilon = 1e-8$, and weight decay multiplier $4.5e-2$. We clip the decompressed gradients by norm using a threshold of 4, prior to applying the Adam update. Gradient clipping is only triggered during the warm-up phase at the start of training. We trained the model using 64 NVIDIA V100 GPUs each with 32GB memory and a total batch size of 256, for a total of 20 epochs, which is about 4K steps. At the start of training, we use a linear schedule to ramp up the learning rate to $1e-4$ over 5000 updates and reduce the learning rate to 0 in a cosine schedule.

Semantic Control Samples

By replacing the visual conditions, we can control the semantics of the generated panoramas. As the cases below, in each sub-figure, the top four images are come from the real view, and will be encoded as semantic condition using CLIP, feeding into our model. When we replace part of the conditions, we can observe that the model will adjust the output to fit the semantic needs (marked with red boxes). Thus we can manipulate and control the panoramas on our needs.



(a)



(b)

More Samples



(c)



(d)



(e)



(f)



(g)



(h)



(i)



(j)



(k)



(l)



(m)



(n)